AD

TECHNICAL REPORT ARCCB-TR-98007

RESIDUAL STRESS IN A SWAGE AUTOFRETTAGED STEEL CYLINDER WITH SEMI-CIRCULAR MID-WALL CHANNELS

S. L. LEE
E. HYLAND
J. NEESE
D. WINDOVER

MAY 1998

US ARMY ARMAMENT RESEARCH,
DEVELOPMENT AND ENGINEERING CENTER
CLOSE COMBAT ARMAMENTS CENTER
BENÉT LABORATORIES
WATERVLIET, N.Y. 12189-4050

DISCLAIMER

The findings in this report are not to be construed as an official Department of the Army position unless so designated by other authorized documents.

The use of trade name(s) and/or manufacturer(s) does not constitute an official indorsement or approval.

DESTRUCTION NOTICE

For classified documents, follow the procedures in DoD 5200.22-M, Industrial Security Manual, Section II-19 or DoD 5200.1-R, Information Security Program Regulation, Chapter IX.

For unclassified, limited documents, destroy by any method that will prevent disclosure of contents or reconstruction of the document.

For unclassified, unlimited documents, destroy when the report is no longer needed. Do not return it to the originator.

REPORT DOCUMENTATION PAGE

Form Approved
OMB No. 0704-0188

1. AGENCY USE ONLY (Leave blank)	2. REPORT DATE	3. REPORT TYPE AND DATES COVERED
	May 1998	Final

4. TITLE AND SUBTITLE

RESIDUAL STRESS IN A SWAGE AUTOFRETTAGED STEEL CYLINDER WITH SEMI-CIRCULAR MID-WALL CHANNELS

5. FUNDING NUMBERS

AMCMS No. 6111.01.91A1.1

6. AUTHOR(S)

S.L. Lee, E. Hyland, J. Neese, and D. Windover

7. PERFORMING ORGANIZATION NAME(S) AND ADDRESS(ES)

U.S. Army ARDEC
Benet Laboratories, AMSTA-AR-CCB-O
Watervliet, NY 12189-4050

8. PERFORMING ORGANIZATION REPORT NUMBER

ARCCB-TR-98007

9. SPONSORING / MONITORING AGENCY NAME(S) AND ADDRESS(ES)

U.S. Army ARDEC
Close Combat Armaments Center
Picatinny Arsenal, NJ 07806-5000

10. SPONSORING / MONITORING AGENCY REPORT NUMBER

11. SUPPLEMENTARY NOTES

Presented at the SEM Spring Conference on Experimental and Applied Mechanics, Bellevue, WA, 2-4 June 1997.
Published in proceedings of the conference.

12a. DISTRIBUTION / AVAILABILITY STATEMENT

Approved for public release; distribution unlimited.

12b. DISTRIBUTION CODE

13. ABSTRACT *(Maximum 200 words)*

X-ray diffraction residual stress distribution analysis was performed for a swage autofrettaged, thick-walled, A723 steel compound cylinder with axial semi-circular mid-wall channels. Because of the existence of high stress gradient components in the stress distribution, the effect of spatial resolution and the x-ray beam spread function were investigated. Experimental stress measurements were compared with results from Tresca's model of a partially autofrettaged solid cylinder. Measured residual stresses were interpreted using an ABAQUS finite element model. Our experimental results verified most features of the predicted hoop stress distribution, including the high stress gradients and compressive stresses near the channel root areas. However, significantly reduced compressive stress levels were observed both near the bore and near the channel roots. An overestimate of fatigue lifetime could result if the reduction of compressive stresses observed experimentally were not taken into account. In solid autofrettaged cylinders, reduction of compressive stresses near the bore has been attributed to the Bauschinger effect. However, there is no analytical model incorporating the Bauschinger effect in the current geometry. This work demonstrated that the introduction of the semi-circular channels in a solid cylinder significantly modified the magnitude and location of stress fields. Both the bore and the channel roots are critical sites for stress concentration. Our analysis further determined that the channel roots were the most critical sites where cracks and failure should occur. Fatigue test results verified that cracking and failure occurred at the channel roots.

14. SUBJECT TERMS

Swage Autofrettage, Perforated Cylinders, Bauschinger Effect, Residual Stress, Finite Element Analysis

15. NUMBER OF PAGES

14

16. PRICE CODE

17. SECURITY CLASSIFICATION OF REPORT	18. SECURITY CLASSIFICATION OF THIS PAGE	19. SECURITY CLASSIFICATION OF ABSTRACT	20. LIMITATION OF ABSTRACT
UNCLASSIFIED	UNCLASSIFIED	UNCLASSIFIED	UL

TABLE OF CONTENTS

LIST OF ILLUSTRATIONS

INTRODUTION

Swage autofrettage is an important manufacturing process for high temperature, high pressure vessels. It entails the operation of driving an oversized mandrel through the interior bore of a cylinder to cause a redistribution of residual stresses within the cylinder. When a cylinder is swage autofrettaged, compressive residual stresses are generated near the cylinder bore to counter the high tensile stresses during operation. The residual stress distribution in swage autofrettaged, thick-walled, solid cylinders has been investigated extensively (refs 1-3), resulting in significantly improved fatigue life.

To design a cylinder with axial perforations for high temperature pressure vessel applications, a compound cylinder was constructed. The compound cylinder consisted of a liner and a jacket, both made from A723 steel. The liner, with semi-circular channels cut at the outer surface, was shrunk fit into the jacket. The unit was then subjected to swage autofrettage to induce favorable residual stresses in order to improve its fatigue life.

Figure 1 displays the upper left portion of a cylinder cross section, showing the location of the mid-wall channels. The "channel root," shown in the figure, is defined as the point on the channel surface that is closest to the bore of the cylinder. The inside diameter (ID), and outside diameter (OD) of the cylinder are labeled. Line OAD defines a direction from the origin of the cylinder through the channel root, and line OEF defines a direction from the origin passing through the mid-point between two channels.

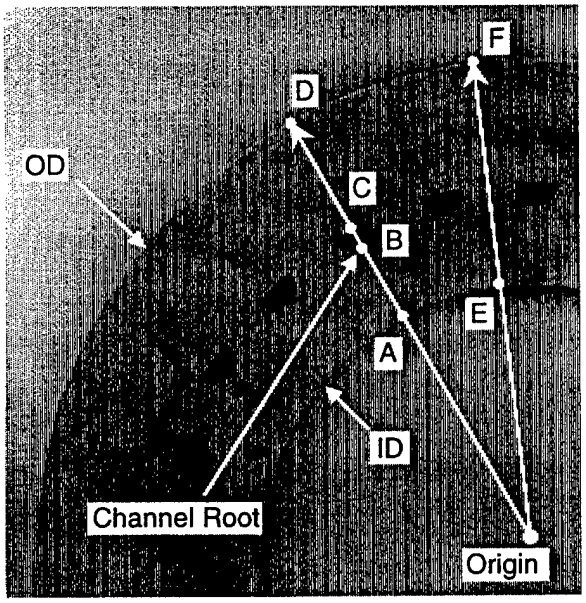

Figure 1. Upper left portion of a cylinder cross section with axial semi-circular channels, showing channel root, ID, OD, and stress measurement paths.

In this work, x-ray residual stress distribution analysis was performed to characterize the effects of axial mid-wall channels. Because there were high gradient components in the residual stress distribution, we investigated the effect of spatial resolution on stress determination and obtained x-ray beam images to determine the effective beam spread. An optimized partial beam technique was used to take experimental measurements in the channel root areas, where high stress gradients were found.

The experimental stress distribution was compared with a model based on Tresca's yield criterion for a solid cylinder under internal pressure. The results were also compared to a two-dimensional, elastic-plastic, finite element deformation model of a perforated cylinder under internal pressure (ref 4). Experimental results verified most of the features predicted by modeling, including the channel root areas where high stress gradients and compressive residual stresses were observed. However, the levels of the hoop compressive stress observed, both near the cylinder bore and at the channel roots, were significantly reduced from model predictions.

The Bauschinger effect reduces yield strength in compression due to a prior tensile plastic overload. In swage autofrettaged, solid cylinders, reduced hoop compressive stresses near the bore, characterized by a hook-like stress distribution, were observed experimentally (refs 2,3). Milligan *et al.* (ref 5) studied the Bauschinger factor dependence on tensile plastic overstrain. Lee *et al.* (refs 2,3) compared experimental residual stresses in a swage autofrettaged cylinder with predictions from an ABAQUS finite element, swage autofrettage model, which predicted a hook. Chen (ref 6) developed a one-dimensional analytical model of a solid cylinder, incorporating both the Bauschinger effect and strain-hardening for a solid cylinder under internal pressure. Then Chen *et al.* (ref 7) made a comparison of this model to the experimental stress distribution. Currently, no analytic model is available to predict the Bauschinger effect in a cylinder of the present geometry, or to determine its effect on the residual stress distribution at the bore and at the channel roots.

The current investigation demonstrated that compared to a solid cylinder, the introduction of mid-wall channels significantly modified the magnitude and location for stress concentrations and altered the potential sites for cracks and failure. Based on our analysis, both the bore and the channel roots are potentially critical sites, with the channel roots being the most critical. When the cylinder was subjected to fatigue testing to failure, all cracks initiated at the channel roots. These cracks grew in a direction perpendicular to the channel surface from the channel roots toward the bore until failure occurred (from point B toward A in Figure 1).

EXPERIMENTAL METHODS

Rings were cut from four autofrettaged cylinders for x-ray evaluation. The cylinders had a ratio of OD to ID of approximately 1.8. Two of the cylinders were fatigue tested and rings were cut from the chamber section. The other two cylinders were not subjected to fatigue testing, and rings were cut closer to the rifling section.

An electropolishing operation was performed using a mixture of sulfuric and phosphoric acids to remove approximately 0.254-mm (10 mils) from the surface of the cross sections. Since the most extensive study was performed on a cylinder that was not subjected to fatigue testing, the results from this cylinder will be reported. A TEC portable stress analyzer equipped with a position-sensitive proportional counter was used to take experimental measurements. Chromium K-α radiation reflected from the {211} peak of martensitic steel at 156.41° 2θ. This reflection was used for x-ray diffraction stress analysis on the cross section of the cylinder. A sample stage, equipped with x and y micrometers, allowed stress measurements at a minimum of 0.025-mm intervals.

RESIDUAL STRESS DISTRIBUTION USING TRESCA'S YIELD CRITERION

For a solid, thick-walled cylinder under internal pressure, residual stress distribution due to the mechanical overstrain may be evaluated based on Tresca's yield criterion, assuming an open-ended condition ($\sigma_z = 0$) (ref 8). The hoop residual stress radial distribution in the plastic region $a \le r \le \rho$ of a partially overstrained cylinder is given by

$$\sigma_{tp} = \sigma_y \{[a^2/(b^2 - a^2)](1 + b^2/r^2)[(\rho^2 - b^2)/2b^2 - \log(\rho/a)] + [(\rho^2 + b^2)/2b^2 - \log(\rho/r)]\} \quad (1)$$

In the elastic region, $\rho \le r \le b$, the hoop residual stress distribution is given by

$$\sigma_{te} = \sigma_y (1 + b^2/r^2)\{(\rho^2/2b^2) + [a^2/(b^2 - a^2)][(\rho^2 - b^2)/2b^2 - \log(\rho/a)]\} \quad (2)$$

where

σ_y	=	yield strength
σ_{tp}	=	hoop stress in plastic zone
σ_{te}	=	hoop stress in elastic zone
a	=	bore radius, b = outside radius
r	=	variable radius, ρ = elastic-plastic interface radius

Figure 2 plots the residual stress predictions from Tresca's model for a solid cylinder under 50, 60, and 70 percent overstrain, assuming a yield strength of 1116 MPa (162 Ksi), showing the elastic and plastic zones.

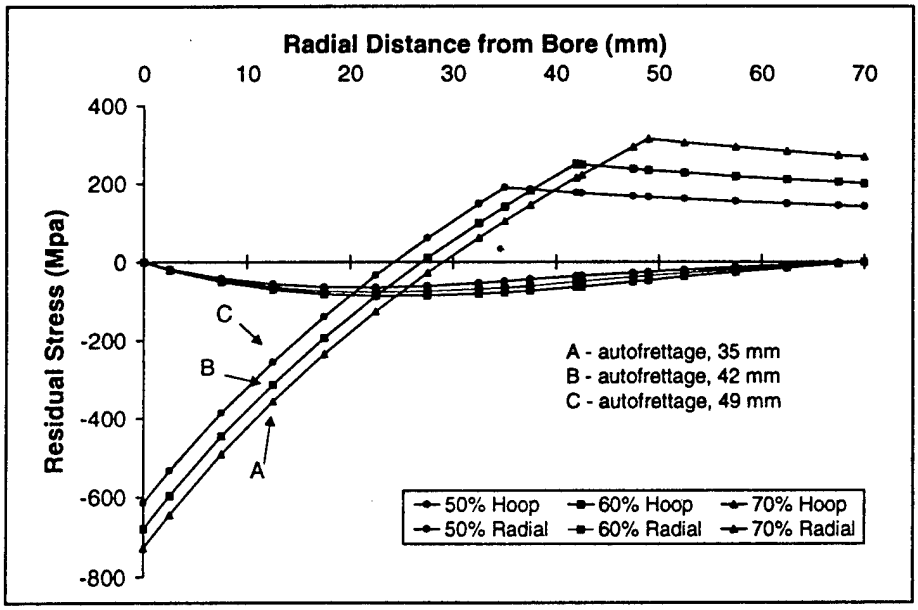

Figure 2. Residual stress distribution using Tresca's yield criterion at 50, 60, 70 percent overstrain of a solid cylinder under internal pressure.

FINITE ELEMENT MODELING

The cylinder consisted of 24 evenly spaced axial channels requiring only a 1/48th section of the cylinder to be modeled by symmetry considerations. A two-dimensional ABAQUS elastic-plastic, quasi-static, finite element model of the perforated cylinder is in progress. Several loading steps have been taken including the autofrettage process, removal of the autofrettage load, load pressure for firing operation, relaxation of the firing pressure, and final residual stress state. Results from this ABAQUS modeling and comparison with experimental measurements are reported in a separate related paper (ref 7).

To predict the structure changes due to the introduction of axial channels, Parker *et al.* (ref 4) performed elastic and elastic-plastic finite element analyses using an alternative mesh, which was biased more toward the channels. This model assumed semi-circular and semi-elliptical channels for a cylinder of similar geometry but slightly different dimension. Figure 3 shows the calculated hoop residual stress radial distribution from the cylinder bore to the channel root for 20, 40, 60, and 80 percent overstrain.

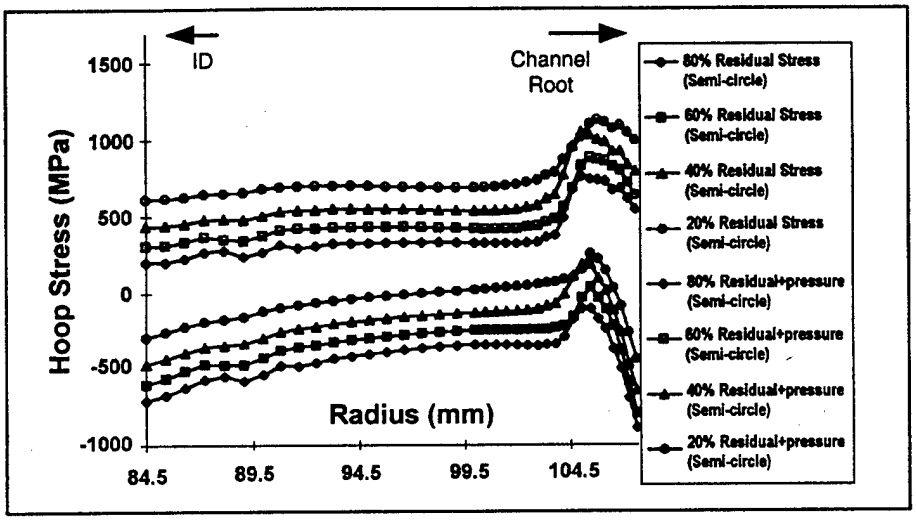

Figure 3. Parker's finite element modeling predictions of hoop residual stress distribution and hoop stress plus bore pressure at 434 MPa from cylinder bore to channel roots at 20, 40, 60, 80 percent overstrain.

High compressive stresses were observed, near the bore, gradually decreasing toward the channel tip. Near the channel root area, a high positive stress gradient was followed by a high negative stress gradient. The lower curves in the figure show maximum hoop compressive residual stresses of -350 to -700 MPa at the bore, and -600 to -900 MPa at the channel roots dependent on the percentage overstrain. The upper curves show residual stress plus bore loading at 434 MPa at various percentages of overstrain. The upper curves also imply that maximum hoop stress occurred at approximately 2-mm from the tip of the channel root, at a magnitude of 600 to 1100 MPa. Failure should occur approximately 2-mm beneath the channel roots.

SIMULATION OF RESOLUTION EFFECT

The predicted residual stress distribution shown in Figure 3 contains high stress gradient components near the channel root areas. Resolution in the x-ray measurement system can significantly affect the accuracy of the measurement of stresses containing high stress gradients. Diffractometer geometry, optical aperture, and range of angles used for the Ψ-tilts define the resolution in an Ω-diffractometer. X-ray stress analysis is based on a linear variation of the lattice spacing d *versus* $\sin^2\Psi$ utilizing multiple Ψ-tilts. Due to the finite size of the slits and collimators, x-ray stress measurement gives the average stress in the irradiated surface area defined by the x-ray beam.

Figure 4 illustrates the effects of three-point averaging and five-point averaging on stress measurement using the predicted stress distribution. The model values come from Figure 3 at 60 percent overstrain. The three-point averaging corresponds to a lateral resolution of 1.2-mm, and the five-point averaging corresponds to a lateral resolution of 2.0-mm. The curves show that the averaging process has a very minor effect on the relatively flat residual stress distribution, but has a major effect when high stress gradients are present, such as at the channel root areas. Measuring system resolution can affect the magnitude of the stresses, and can shift the maximum stress peaks causing erroneous stress measurements. In this work, optimized collimator diameters and slit widths were used to perform the measurements.

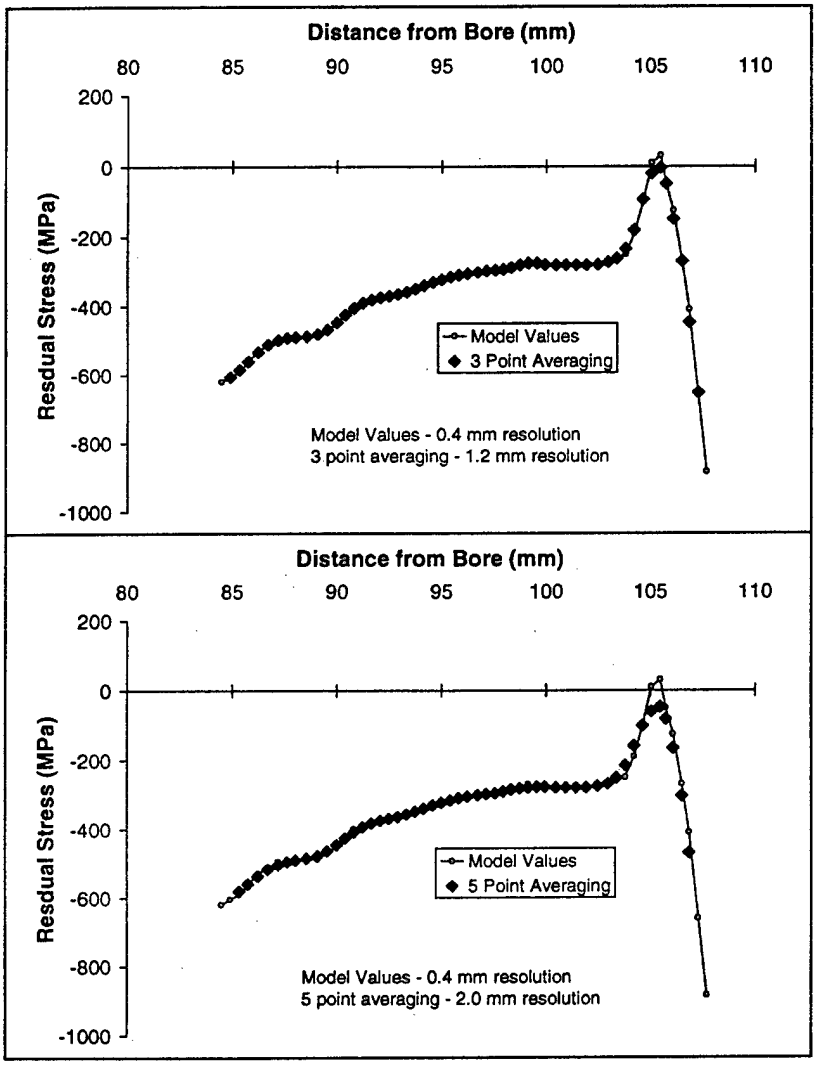

Figure 4. Simulation of resolution effect in x-ray stress analysis for a residual stress distribution containing high stress gradients. Top graph illustrates three-point averaging of Figure 3 data. Bottom shows five-point averaging.

X-RAY BEAM SPREAD FUNCTION

The TEC stress analyzer utilizes a divergent beam geometry, with 30-mm long collimators and slits to define the beam. The x-ray beam can be considered almost parallel. The beam-spread function for various diameter collimators and slit widths was investigated by exposing x-ray films under the beam at various Ψ-tilts. Figure 5 shows similar TEC images of collimators and slits at Ψ = -45°, 0°, 45° using a cross wire (ref 9). Very slight beam spreading in the lateral direction was observed. For a 1-mm diameter collimator, lateral resolution stayed at 1 to 1.1-mm. In the vertical direction, a slightly larger beam spread can be expected. This spread is intrinsic to the $\sin^2\Psi$ method, and the magnitude of the spread depends on the size of the collimator, slit, and the Ψ scan range used. The vertical beam spread would be small compared to the theoretical stress gradients in the vertical direction near the channel roots.

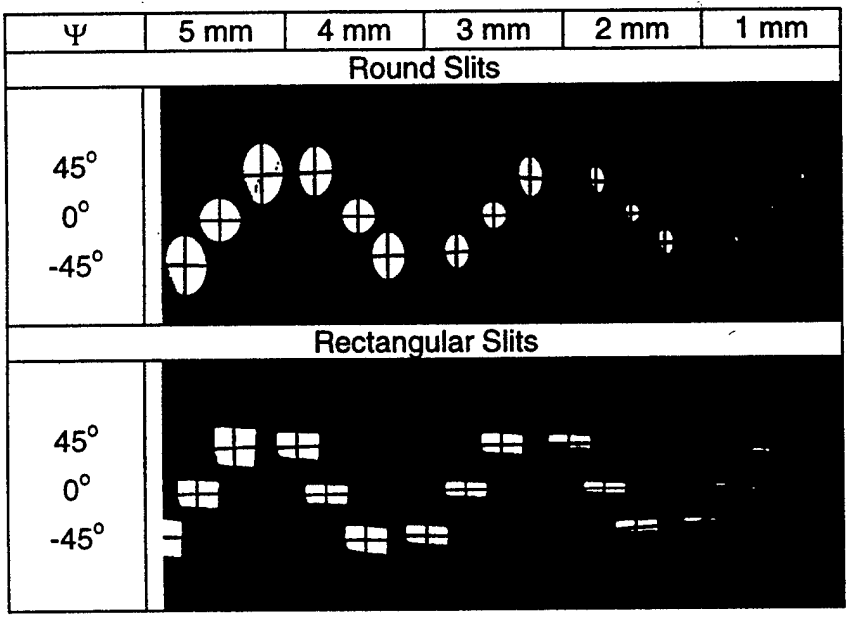

Figure 5. Lateral (horizontal) and vertical x-ray beam spread function.

X-RAY RESIDUAL STRESS FROM ID TO OD (NO IMMEDIATE CHANNEL ROOT AREAS)

A finite element modeling study of the effect due to slicing has been conducted by O'Hara (ref 10). Results showed that the slicing effect decreases with increasing slice thickness. This effect should be small for the slices under investigation due to their thickness. Optimized collimators of 0.5-mm and 1-mm diameter were used for data acquisition. A partial beam technique described below was necessary to take stress measurements in the channel root areas.

Directions OAD and OEF are defined in Figure 1. Figure 6 depicts the radial distribution of hoop residual stresses, from ID to OD, along these directions. The figure shows that compressive residual stresses near the bore at -600 MPa gradually diminished, and turned to slightly tensile at 80 MPa near the channel root. Measured stress abruptly changed to compressive stress at the channel root with only one data point of -100 MPa. The maximum compressive stress near the bore was -750 MPa and occurred approximately 3-mm from the bore. The decreased compressive stresses near the bore were similar to stresses observed in solid cylinders. When comparing modeling hoop stresses in Figure 3 to experimental stresses in Figure 6, good agreement was reached. Deviations occurred at the bore and at the channel roots, where reduced compressive stresses were observed. In the outer jacket, residual stress was mostly tensile, between approximately 100 to 250 MPa.

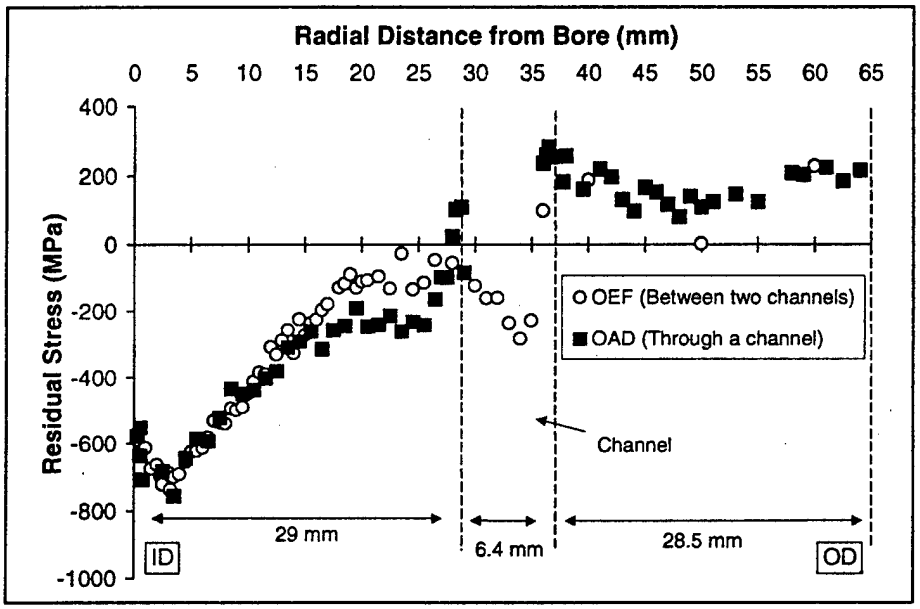

Figure 6. X-ray hoop residual stress distribution along paths OAD and OEF from cylinder bore to OD (without detailed analysis for the channel root areas).

Mid-channel stresses along direction OEF were similar to stresses along OAD, with noted differences when approaching the channel root areas. Note also that the mid-channel stresses changed abruptly at the liner-jacket interface from -300 MPa in the liner to 100 MPa in the jacket. There was a long range of relatively flat compressive stress distribution left of the channel root, approximately 13 to 25-mm from the bore, which helped to arrest cracks from further growth.

EXPERIMENTAL DATA COMPARED TO TRESCA'S MODEL

Figure 2 shows the stress distribution predicted from Tresca's yield criterion for a solid cylinder of the same ID and OD dimension under 50, 60 and 70 percent overstrain. Figure 7 shows Tresca stresses at 60 percent overstrain compared with experimental stress measurements. The triangles represent raw experimental data, while the solid line is Tresca's curve. The comparison shows fairly good agreement except near the bore and the channel roots.

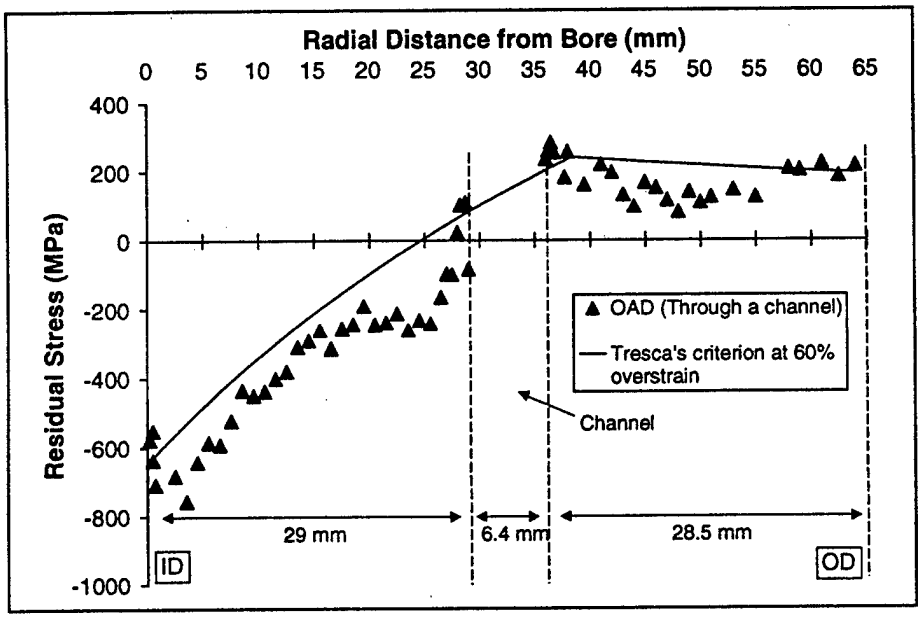

Figure 7. Comparison of experimental residual stress distribution along OAD from ID to OD with Tresca's solid cylinder 60 percent overstrain.

RESIDUAL STRESS BORE TO CHANNEL ROOT USING A PARTIAL BEAM TECHNIQUE

Figure 8 shows the residual stress at critical locations A, B, C, and D, representing the bore, the channel root, the channel top, and OD, respectively. The residual stress can be measured using an unconventional partial beam technique. However, a full x-ray beam is generally recommended to perform x-ray stress analysis. The partial beam technique requires monitoring of the reflected beam intensity, overriding the system low-count rate limit; it also requires extra shielding for possible stray x-rays due to the vertical surfaces inside the channel walls. This method is suited for the channel root areas where high stress gradients and high radius of curvature make conventional residual stress measurements difficult. Errors of 100 MPa (15 Ksi) would be expected depending on the percentage of the beam used in the measurement. In normal x-ray analysis, errors of 35 MPa (5 Ksi) would be expected.

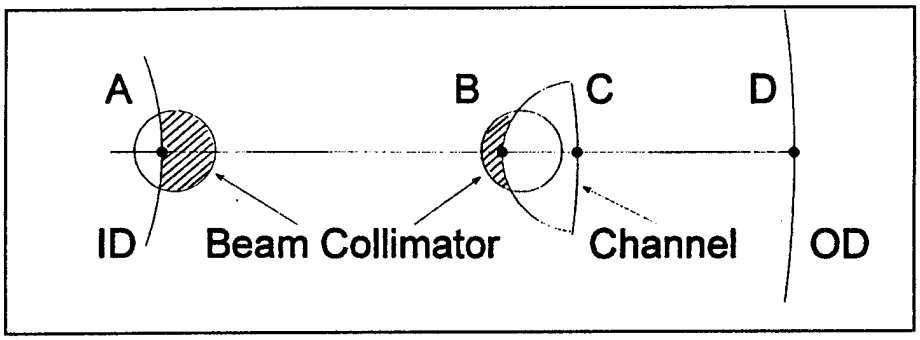

Figure 8. Geometry of the experimental set-up for x-ray measurements at cylinder bore A, channel root B, channel top C, and at outside diameter D using a partial beam technique.

The open squares in Figure 9 illustrate hoop residual stress from bore to channel root using the partial beam technique. The data were taken from a different channel than that used in Figure 6. Compressive stresses of -550 MPa near the bore decreased in magnitude, turning slightly tensile at 100 MPa near the channel root, and then abruptly turning into compressive stresses. The maximum compressive stress measured at the channel root was -200 MPa. The stress distribution curves from bore to channel root in Figures 6 and 9 were similar. However, Figure 9 shows a less pronounced Bauschinger effect near the bore, with the number of measurement points at the channel root extended. A theoretical ascending slope of 200 MPa/mm (29 Ksi/mm) and a descending slope of -345 MPa/mm (-51 Ksi/mm) were obtained from Figure 3. The measured experimental ascending slope was 220 MPa/mm (32 Ksi/mm) and the descending slope was -282 MPa/mm (-41 Ksi/mm).

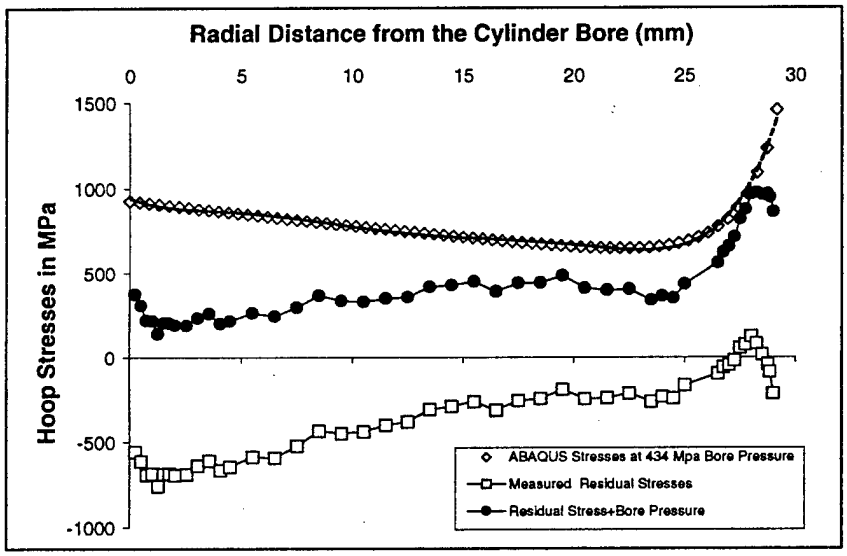

Figure 9. Residual stress from cylinder bore to channel root using optimized collimator and slit, and a partial beam technique.

A comparison of residual stress levels in Figures 3, 6, and 9 showed that observed residual stresses were much less than predicted at the cylinder bore and at the channel roots. The measured reduction in compressive stress at the bore compared to the maximum residual stress was 200 MPa. The maximum compressive stresses occurred approximately 2 to 3-mm from the bore. This reduced bore stress has been attributed to the Bauschinger effect, not included in Parker's model.

FATIGUE TEST RESULTS

Operational stresses superimpose on the locked-in residual stresses to determine the safety operation and fatigue life of a component. Current residual stress analysis indicates that cracks should be expected to initiate at subsurfaces just beneath the channel roots, where residual stress plus bore pressure is the most tensile. However, from experience, cracks always initiate at surfaces.

The cylinder, which was fatigue tested to failure, was cut and examined by magnetic particle inspection and by visual observation. When it was cut into slices, cracks were observed. All of the cracks initiated at or near the center of the channel root areas of the liner. The cracks grew in a direction perpendicular to the surface of the channel toward the bore, direction BA in Figure 1, until complete failure of the unit.

RESIDUAL STRESS EFFECTS

From a residual stress point of view, the bore and the channel roots are competing locations of stress concentration. The current investigation determined that compressive stress levels were much greater at the bore than at the channel roots. The open diamonds in Figure 9 are the most recent ABACUS hoop stresses in the perforated cylinder under 434 MPa bore pressure (ref 7). The black circles in Figure 9 show combined residual stress with operational bore pressure. These data show the channel roots are the most critical sites for cracks and failure. Cracks initiated at the channel because residual stress superimposed on the operational stress was tensile. Furthermore, tensile stresses immediately under the channel root surface helped the cracks grow farther, leading to failure of the component.

At the channel root, observed stresses of -300 MPa were significantly lower than the predicted stresses of -800 MPa for 60 percent overstrain. The 500 MPa difference could modify the upper curves in Figure 3, which represent residual stress plus bore pressure. This change could make the stress more tensile at the channel roots, and failure would be more likely to occur at the channel roots than at the bore. It could also shift the maximum tensile stress in Figure 3 toward the channel root, making failure closer to the surface more likely.

CONCLUSIONS

- Experimental residual stress analysis was performed to characterize the effects of axial semi-circular channels in a swage autofrettaged cylinder.

- Due to the high stress gradient components at the channel roots, a partial beam technique was used to acquire data near the channel root areas.

- Experimental results showed good comparison with calculated hoop and radial residual stress distribution, assuming Tresca's yield criterion for a solid cylinder under internal pressure.

- Experimental measurements were also in good agreement with predictions from a finite element, elastic-plastic deformation model by Parker. Observed compressive stress levels were significantly reduced from model predictions at the bore and the channel roots. If the measured reduced compressive levels were not taken into account, they could lead to an overestimate of fatigue lifetime.

- A comparison to modeling predictions led to the conclusion that the Bauschinger effect plays an important role near the bore, but its effect at the channel root is unknown.

- Based on the present analysis, the channel roots and the bore are competing sites for stress concentrations. Residual stress analysis determined that the channel roots are the most critical sites in the design and safety operation of the component.

- Fatigue test results showed that cracks initiated at the channel roots and grew in the liner toward the bore until failure.

REFERENCES

1. Clark, G., "Residual Stresses in Swage-Autofrettaged Thick-Walled Cylinders," Materials Research Laboratories Report MRL-R-847, 1982.

2. Lee, S.L., O'Hara, G.P., Olmstead, V., and Capsimalis, G., "Characterization of Residual Stresses in an Eccentric Swage Autofrettaged Thick-Walled Steel Cylinder," *Proceedings of ASM International Conference on Practical Applications of Residual Stress Technology*, 1991, pp. 123-129.

3. Lee, S.L., Britt L., and Capsimalis, G., "Comparison of Residual Stress and Hardness in a Symmetric and an Eccentric Swage Autofrettaged Cylinder," *Nondestructive Characterization of Materials VI*, Plenum Press, 1994, pp. 425-434.

4. Parker, A.P., Endersby, S.N., Bond, T. J., Underwood, J.H., Lee, S.L., and Higgins, J., "Stress Concentration, Stress Intensity, and Fatigue Lifetime Calculations in Autofrettaged Tubes Containing Axial Perforations Within the Wall," *Trans. ASME, Journal of Pressure Vessel Technology*, Vol 119, 1997, pp. 488-493.

5. Milligan, R.V., Koo, W.H., and Davidson, T.E., "The Bauschinger Effect in a High-Strength Steel," *Trans. ASME, Journal of Basic Engineering,* Vol. 88, June 1966, pp. 480-488.

6. Chen, P., "Stress and Deformation Analysis of Autofrettaged High Pressure Vessels," *ASME Pressure Vessels and Piping Conference*, PVP Vol 110, 1986, pp. 61-67.

7. Chen, P., Leach, M., and Lee, S.L., "Modeling and Measurement of Residual Stresses in a Swage Autofrettaged Cylinder with Axial Perforations," *Abstract Proceedings of 1998 SEM Spring Conference*, 1-3 June 1998.

8. Davidson, T.E., Kendall, D.P., and Reiner, A.N., "Residual Stresses in Thick-Walled Cylinders Resulting from Mechanically Induced Overstrain," *Experimental Mechanics*, November 1963.

9. TEC Model 1600 Stress Analyzer Systems Acceptance Test Procedure, QCTP-138, 1990.

10. O'Hara, P., Private Communication, Benet Laboratories, Watervliet, NY, 1997.

TECHNICAL REPORT INTERNAL DISTRIBUTION LIST

	NO. OF COPIES
CHIEF, DEVELOPMENT ENGINEERING DIVISION	
ATTN: AMSTA-AR-CCB-DA	1
-DB	1
-DC	1
-DD	1
-DE	1
CHIEF, ENGINEERING DIVISION	
ATTN: AMSTA-AR-CCB-E	1
-EA	1
-EB	1
-EC	1
CHIEF, TECHNOLOGY DIVISION	
ATTN: AMSTA-AR-CCB-T	2
-TA	1
-TB	1
-TC	1
TECHNICAL LIBRARY	
ATTN: AMSTA-AR-CCB-O	5
TECHNICAL PUBLICATIONS & EDITING SECTION	
ATTN: AMSTA-AR-CCB-O	3
OPERATIONS DIRECTORATE	
ATTN: SIOWV-ODP-P	1
DIRECTOR, PROCUREMENT & CONTRACTING DIRECTORATE	
ATTN: SIOWV-PP	1
DIRECTOR, PRODUCT ASSURANCE & TEST DIRECTORATE	
ATTN: SIOWV-QA	1

NOTE: PLEASE NOTIFY DIRECTOR, BENÉT LABORATORIES, ATTN: AMSTA-AR-CCB-O OF ADDRESS CHANGES.

TECHNICAL REPORT EXTERNAL DISTRIBUTION LIST

	NO. OF COPIES
ASST SEC OF THE ARMY RESEARCH AND DEVELOPMENT ATTN: DEPT FOR SCI AND TECH THE PENTAGON WASHINGTON, D.C. 20310-0103	1
DEFENSE TECHNICAL INFO CENTER ATTN: DTIC-OCP (ACQUISITIONS) 8725 JOHN J. KINGMAN ROAD STE 0944 FT. BELVOIR, VA 22060-6218	2
COMMANDER U.S. ARMY ARDEC ATTN: AMSTA-AR-AEE, BLDG. 3022 AMSTA-AR-AES, BLDG. 321 AMSTA-AR-AET-O, BLDG. 183 AMSTA-AR-FSA, BLDG. 354 AMSTA-AR-FSM-E AMSTA-AR-FSS-D, BLDG. 94 AMSTA-AR-IMC, BLDG. 59 PICATINNY ARSENAL, NJ 07806-5000	 1 1 1 1 1 1 2
DIRECTOR U.S. ARMY RESEARCH LABORATORY ATTN: AMSRL-DD-T, BLDG. 305 ABERDEEN PROVING GROUND, MD 21005-5066	1
DIRECTOR U.S. ARMY RESEARCH LABORATORY ATTN: AMSRL-WT-PD (DR. B. BURNS) ABERDEEN PROVING GROUND, MD 21005-5066	1
COMMANDER ROCK ISLAND ARSENAL ATTN: SMCRI-SEM ROCK ISLAND, IL 61299-5001	1
COMMANDER U.S. ARMY TANK-AUTMV R&D COMMAND ATTN: AMSTA-DDL (TECH LIBRARY) WARREN, MI 48397-5000	1
COMMANDER U.S. MILITARY ACADEMY ATTN: DEPARTMENT OF MECHANICS WEST POINT, NY 10966-1792	1
U.S. ARMY MISSILE COMMAND REDSTONE SCIENTIFIC INFO CENTER ATTN: AMSMI-RD-CS-R/DOCUMENTS BLDG. 4484 REDSTONE ARSENAL, AL 35898-5241	2
COMMANDER U.S. ARMY FOREIGN SCI & TECH CENTER ATTN: DRXST-SD 220 7TH STREET, N.E. CHARLOTTESVILLE, VA 22901	1
COMMANDER U.S. ARMY LABCOM, ISA ATTN: SLCIS-IM-TL 2800 POWER MILL ROAD ADELPHI, MD 20783-1145	1

NOTE: PLEASE NOTIFY COMMANDER, ARMAMENT RESEARCH, DEVELOPMENT, AND ENGINEERING CENTER, BENÉT LABORATORIES, CCAC, U.S. ARMY TANK-AUTOMOTIVE AND ARMAMENTS COMMAND, AMSTA-AR-CCB-O, WATERVLIET, NY 12189-4050 OF ADDRESS CHANGES.

TECHNICAL REPORT EXTERNAL DISTRIBUTION LIST (CONT'D)

	NO. OF COPIES
COMMANDER U.S. ARMY RESEARCH OFFICE ATTN: CHIEF, IPO P.O. BOX 12211 RESEARCH TRIANGLE PARK, NC 27709-2211	1
DIRECTOR U.S. NAVAL RESEARCH LABORATORY ATTN: MATERIALS SCI & TECH DIV WASHINGTON, D.C. 20375	1
WRIGHT LABORATORY ARMAMENT DIRECTORATE ATTN: WL/MNM EGLIN AFB, FL 32542-6810	1
WRIGHT LABORATORY ARMAMENT DIRECTORATE ATTN: WL/MNMF EGLIN AFB, FL 32542-6810	1

NOTE: PLEASE NOTIFY COMMANDER, ARMAMENT RESEARCH, DEVELOPMENT, AND ENGINEERING CENTER, BENÉT LABORATORIES, CCAC, U.S. ARMY TANK-AUTOMOTIVE AND ARMAMENTS COMMAND, AMSTA-AR-CCB-O, WATERVLIET, NY 12189-4050 OF ADDRESS CHANGES.